

Document downloaded from:

<http://hdl.handle.net/10251/37663>

This paper must be cited as:

Bañuls Polo, MJ.; Puchades Pla, R.; Angel Maquieira Catala (2013). Chemical Surface Modifications development of Silicon Based Label Free Integrated Optical (IO) Biosensors: A Review. *Analytica Chimica Acta*. 777:1-16. doi:10.1016/j.aca.2013.01.025.



The final publication is available at

<http://dx.doi.org/10.1016/j.aca.2013.01.025>

Copyright Elsevier Masson

24	Contents
25	1. Introduction. Approach to Refractive Index Optical BioSensors
26	2. Surface Chemistry Approaches for Bioreceptor Attachment on Silicon-Based
27	Materials
28	2.1. Chemical Surface Modifications and Bioreceptors Attachment
29	2.1.1. Chemical Surface Modification by Self-Assembled Silane-Based
30	Layers
31	2.1.2. Other Silicon Surface Chemical Modifications
32	2.1.3. Capture Agents employed as Model Systems
33	2.2. Techniques Employed for the Biofunctionalization of IO Devices
34	2.3 Characterization Techniques for Modified Surfaces
35	3. Performance and Applications. Main Achievements
36	4. Future Trends
37	References
38	
39	
40	

41 **1. Introduction. Approach to Refractive Index Optical BioSensors**

42 Nowadays, biosensing is a scientific and technological hot topic given its potential in
43 fields such as medical diagnosis, healthcare, environment, defense and food security. In
44 these realms, the specific and sensitive detection of targets in short-time analyses plays
45 a primordial role.

46 Traditionally, labeled formats have been used, where targets or reporter molecules
47 carry fluorescent, enzymatic or radioactive tags. These techniques present high
48 sensitivity, and even achieve single molecule detection [1], and are currently the
49 standard techniques for many determinations. However, the development of label-free
50 techniques has attracted the interest of many researchers over the last decade [2-6].
51 They offer advantages such as direct detection, real-time monitoring, kinetic
52 information, fewer reagent costs, and the native molecular conformation of the protein
53 is not altered by a tag. Thus, label-free biosensors based on optical [7], electrical [8-13]
54 and mechanical principles [14-18] can be found. Optical sensors are more versatile than
55 others because they can be made from different materials, such as silicon, glass, metals
56 or polymers, and they offer different detection modes and architectures that can be
57 combined [19]. They also offer other advantages; mass-scale fabrication, excellent
58 physical properties, good selectivity and sensitivity; and can accomplish multiplexed
59 detection in a single device [20,21]. Label-free optical biosensors have received
60 increasing attention and many reviews can be found that provide a general overview of
61 the state of the art [22-25]. In label-free optical detection, the transduction mode may be
62 based on the refractive index (RI), optical absorption or Raman spectroscopy [26-30]. In
63 past two decades, optical sensors based on refractive index (RI) changes feature among
64 the most studied (Figure 1).

65 In ordinary dielectric material, the refractive index (RI) directly relates to the
66 polarizability of molecules at optical wavelengths. Biological molecules have a higher
67 RI than air or water, and they lower the propagation speed of the electromagnetic fields
68 passing through them. Optical biosensors are designed to translate changes in the
69 propagation velocity of light through a medium that contains biological material into a
70 quantifiable signal proportional to the amount of material present on the sensor surface.
71 For this reason, the electromagnetic field bound to an optical device that couples some
72 energy to an external medium (called an evanescent field) penetrates a few hundred
73 nanometers into the optically rarer environment from the optically denser guiding
74 medium.

75 Different optical phenomena have been employed to design RI optical biosensors.
76 Representative methods include: Surface Plasmon Resonance [31,32], Reflectometric
77 Interference Spectroscopy [33,34], Dual polarization Interferometry [35,36], Photonic
78 Crystal Technology [37,38], and Whispering Gallery Mode Resonators [39,40].
79 Extensive reviews have been written and detail all these approaches which have
80 developed to act as biosensors [25, 39, 40, 41].

81 The search for analytical platforms that operate rapidly and efficiently has received
82 increasing interest in recent years, not only for RI optical biosensors in particular, but
83 also for label-free biosensors in general [42,43]. Optical label-free biosensors are ideal
84 candidates for lab-on-a-chip (LOC) applications [41,44,45] as they allow the integration
85 of both fluidic handling and optical analyses into a single chip. These integrated sensing
86 devices enable the mass production of high-density biosensors, and provide rapid,
87 sensitive and multiplexed measurements at the required point. Integrated Optical (IO)
88 Biosensors employ guided waves or modes in planar optical waveguides. Besides
89 Silicon-on-Insulator (SOI) technology, waveguide materials usually include high

90 refractivity silicon dioxide or titanium dioxide and silicon nitride films in oxidized
91 silicon wafer substrates.

92 A number of different IO biosensors has been designed and significant advances have
93 been made in label-free interferometric [46], grating-coupled [47,48], photonic crystals
94 [37,38,39] and microcavity resonators [39,40,49-52] biosensors.

95 Within waveguiding interferometers, Mach-Zehnder [44,53-55], and in a less extent
96 Young interferometers [56,57] are used mainly for biosensing, although novel
97 interferometric designs with improved performance are being continuously explored
98 [58-60].

99 The materials used to construct integrated interferometers for biosensing include
100 mainly silicon oxide, silicon nitride, SOI and, to a lesser extent, polymers.

101 Grating coupled sensors are made from SiO_2 , Ta_2O_5 and $\text{SiO}_2/\text{TiO}_2$ on glass
102 substrates, and they rely on the phenomenon that the coupling of light of a certain
103 wavelength into a planar optical waveguide via grating occurs only at a critical
104 incidence angle. The measurement principle can be Optical Waveguide Lightmode
105 Spectroscopy (OWLS) [47] or Wavelength Interrogated Optical Systems (WIOS)
106 [61,62].

107 Photonic crystals (PhC) are dielectric structures whose periodicity is in the order of a
108 wavelength. The frequency of light that is coupled into PhC depends on the RI in the
109 local environment around an introduced defect, which acts as a transduction signal
110 when biorecognition takes place [63]. In other designs [38,64], binding events shift the
111 wavelength of the reflected light proportionally to the adsorbed mass.

112 Another emerging class of miniaturized optical resonators, which reach exceptionally
113 high-quality Q-factors, are the Whispering Gallery Mode resonators [65]. To date, they
114 have been implemented into three major configurations: microfabricated rings, disks

115 and toroids [39,41], stand-alone microspheres [66,67], and capillary-based optofluidic
116 ring resonators (OFRs) [68]. Among them, silica micro disks, rings and toroids are
117 preferred for IO devices.

118 An excellent overview on the recent developments in resonant microcavities and
119 photonic crystals for chemical and biological analysis was recently published by
120 Luchansky and Bailey [39].

121 Other highly sensitive label-free biosensors based on optical fibers also exist [69].
122 However, they need external optical components that are not integrated into the chip, as
123 well as larger sample volumes. Therefore, miniaturized optical devices are preferred for
124 portable applications that also include LOC architectures.

125 Two points are key to construct IO biosensors: optofluidic integration [25,39,41,70-
126 72] and device biofunctionalization. Regarding functionalization, and although
127 everyone agrees on the importance of proper surface functionalization to provide
128 selectivity and good sensitivity, systematic studies into the biofunctionalization
129 processes employed in these devices are lacking. Such methodologies are generally
130 based on the same principle, but there is disagreement about procedures, and treated
131 surfaces are often poorly characterized. Because silicon technology appears to be the
132 choice currently preferred for the majority of IO biosensors, the biofunctionalization
133 chemistries employed in the sensors constructed on silicon-based materials are
134 discussed in the next section.

135 Surface modification of planar silicon-based substrates, with covalently linked
136 organic monolayers, has been extensively studied [73-76]. In addition, the literature
137 describes organic surface modification of silicon nanowires for sensing [77,78].

138 This review is an overview of all the different surface modification strategies
139 explored to functionalize Si-based IO biosensors, and it discusses the bioreceptors and

140 methodologies employed, the techniques available for surface characterization, and the
141 main achievements accomplished in real biosensing.
142

143 2. Surface Chemistry Approaches for Bioreceptor Attachment on Silicon-Based

144 Materials

145 2.1. Chemical Surface Modifications and Bioreceptors Attachment

146 The specific detection of analytes is based on the immobilization of a bioreceptor that
147 interacts with the target of interest. Immobilization can be done in two ways: direct
148 adsorption; covalent, electrostatic or affinity binding. In all cases, it is necessary to
149 modify the surface of the support material to the extent that the material properties are
150 tuned to accomplish the best analytical characteristics. Performance comprises: favoring
151 the receptor attachment that induces selectivity to a target of interest; preventing surface
152 fouling; changing the hydrophobicity/hydrophilicity of the surface, while maintaining
153 the sensing system's physical (optical, mechanical, etc.) properties.

154 Although bioreceptor physisorption has been widely used, especially for the
155 preliminary demonstrations of new optical sensors designs [79-87], it has several
156 drawbacks, which include: random orientation, lack of reproducibility, long incubation
157 times, and risk of folding and desorption when the receptor is adsorbed. This issue is
158 very important when working in flow and when chip regeneration is desired. In such
159 cases, the covalent attachment of receptors is recommended.

160 Ideally, biofunctionalization chemistries should fit the following requirements: gentle
161 enough to avoid the structural damage of both the receptor and the transducer; few
162 reaction steps; low optical adsorption at the working wavelengths; homogeneously thin
163 layer formation that is compatible with evanescent field sensing; good surface coverage;
164 reproducibility; robustness; low non specific binding; minimal sample and reagents
165 consumption; easy handling; biocompatible conditions (pH, ionic strength, solvent,
166 etc.); integrability with mass-scale fabrication.

167 Selecting a proper immobilization technique is a key point as many factors can
168 negatively affect final biosensor performance. Several aspects, such as orientation and
169 probe density on the surface, pH, target concentration, matrix effects, operating
170 conditions and impact of the targeting strategy on transducer sensitivity, must be
171 carefully analyzed.

172 Figure 2 represents the main functionalization approaches employed to construct IO
173 biosensors.

174 *2.1.1. Chemical Surface Modification by Self-Assembled Silane-Based Layers*

175 Most of the methods applied to functionalize silicon surfaces employ the self-
176 assembly of organofunctional alkoxy-silanes (Figure 2a). This strategy assumes standard
177 glass-based surface functionalization chemistry, and is well-suited to the
178 functionalization of silica-on-silicon optical devices. The reaction is based on the
179 condensation between the siloxanes of the organosilane and hydroxyl moieties present
180 on the surface. Thus, the density of silanol groups is a determinant to form a proper
181 organic layer. In the case of silicon and silicon nitride materials, the hydroxyl groups
182 derive from the native silicon oxide layer, which is always present, although etching the
183 native layer and forming a new one, usually by thermal oxidation, is commonplace [88-
184 92].

185 The formation of silane self-assembled monolayers (SAMs) is more complex than the
186 assembly of thiol molecules on gold surfaces. Yet it offers one important advantage in
187 that silane-terminated monolayers show higher physical and chemical stability as
188 opposed to thiol-ended ones. Therefore, it is possible to apply a large pool of chemical
189 reactions. Alkylsiloxane monolayers are usually prepared by a chemisorption process of
190 self-assembling molecules, such as trichloro-, trimethoxy- or triethoxysilanes, onto the
191 solid substrate [93]. Despite the formation mechanism having been extensively

192 investigated, there is still some controversy [94-95]. It is well-known that certain
193 parameters, such as water content, solvent use, age of the solution, deposition time and
194 temperature, are still largely depended on [96]. In our opinion, not enough attention is
195 paid to these issues. Frequently, the reaction conditions are established randomly, as
196 evidenced by the fact that different concentrations, solvents (from aqueous ethanol to
197 anhydrous toluene), reaction times or temperatures are employed for the same
198 organosilane, by assuming that a monolayer is formed.

199 Immediately before silanization, surfaces are cleaned with oxidant media to remove
200 organic pollutants and to increase the hydroxyl moieties on the surface ($\approx 10^{15}$ per cm^2)
201 [73]. A cleaning process to generate reactive hydroxyl groups is critical for the effective
202 immobilization of silanes. There are several types of Si-OH groups that can be formed
203 on silica surfaces. Some (germinal and isolated silanols) are reactive, whereas others
204 (the vicinal silanol and siloxane groups) are not. The most widely used oxidants are
205 oxygen plasma [97-103] and piranha solution [63, 104-111], consisting of a
206 concentrated sulfuric acid: a hydrogen peroxide mixture at different ratios varying from
207 3:1 to 7:3. This treatment is well-performed at room temperature or by heating, but
208 usually for only a few minutes. The literature also describes other oxidants and cleaning
209 agents comprising ozone-UV [112], sodium hydroxide [113], the ammonia:hydrogen
210 peroxide mixture [114,115], nitric acid [53,116], hydrochloric acid [117], sulfuric acid
211 [118], chromic acid [119], or mineral acids with hydrogen peroxide [115]. Sometimes
212 more than one of these treatments is combined and sequentially applied to the chip
213 [115,117,120,121].

214 Our group compared the two mostly used oxidation protocols -oxygen plasma and
215 piranha treatment- using planar silica chips. In both cases, the water contact angle
216 became 0° after the oxidation step (36° before oxidation), indicating the large number of

217 hydroxyl groups created on the surface. Afterward, the organosilane layer formed using
218 3-aminopropyltriethoxysilane (APTES) provided similar results for both procedures.

219 Piranha solution was also used to regenerate the surface. However, our experience
220 indicates that the best procedure must be evaluated in each case; thus, we found the
221 piranha treatment was the most suitable for silicon and silicon nitride materials, while a
222 chromic mixture was the best choice for silicon oxynitride surfaces. Furthermore, the
223 number of feasible regenerations on the same surface is limited and has to be evaluated
224 experimentally. Our studies have found that the number of regeneration cycles ranges
225 from three to five.

226 Among the vast variety of commercially available organosilanes [122], very few have
227 been used to functionalize IO transducers. In our opinion, there are two reasons for this:
228 first, short alkyl chains are preferred as the evanescent field decays with distance from
229 the surface; second, the methods are adopted from the well-established glass-based
230 bioconjugation methods employed in biochips. Thus, $-NH_2$, $-SH$, $-COOH$, or epoxy
231 functionalities, are mainly employed [123].

232 The methods applied for the biofunctionalization of silicon-based IO biosensors are
233 discussed according to the terminal functionality of the organosilane used. The
234 bioconjugation protocol following organosilane layer assembly is also critically
235 presented.

236 *NH₂ organosilane*

237 Given its reactivity to aldehyde, carboxylic acid and epoxy functionalities, APTES (3-
238 aminopropyltriethoxysilane) [53,63,89-92, 107-110,97, 100,103, 112,
239 114,116,120,124,125-127] and APTMS (3-aminopropyltrimethoxysilane)
240 [88,111,98,99,128] have become the most widely used linker compounds for
241 biofunctionalization purposes (Figure 3). However, the conditions employed differ for

242 silane concentration, solvent and incubation time. Moreover, a curing process is often
243 performed after silanization. The trimethoxy compound is more reactive and can be
244 deposited on a substrate using 100% pure organic solvent. The advantage of this process
245 is that a thinner, and a more controlled deposition of the silane, can be generated to
246 create a monolayer of the aminopropyl groups on the surface. For triethoxysilane, the
247 reaction must occur in the presence of water, otherwise the ethoxy groups are not
248 reactive enough to spontaneously couple to the hydroxyl groups on the surface.

249 Given the possibility of hydrogen bond formation between the amine of APTES and
250 the SiO_x surface, both the head and tail groups in the organosilane can be oriented
251 toward the surface, which can result in a disordered layer [126]. Additionally, cross-
252 linking among alkoxy silane units may yield oligomerized silane structures, resulting in
253 rough layers that are thicker than a monolayer. The optimal conditions for solvent-based
254 silanization using APTES have been investigated on planar surfaces [96]. Experiments
255 with a 1% APTES concentration provide good films where the reaction time was less
256 than 1 h, and the APTES film becomes thicker with longer reaction times.

257 Having aminated the surface, different procedures are employed to attach the probe.
258 An aminated surface is used to directly immobilize antibodies by adsorption
259 [53,125,127] or to covalently attach an N-hydroxysuccinimide ester-ended biotin (NHS-
260 bt) (Figure 3a) [88,97-100,103,110,111,112,114,116,128]. NHS esters bind in nearly
261 quantitative yields with primary amines, resulting in the formation of a stable amide
262 bond. However, NHS esters typically undergo rapid hydrolysis under aqueous
263 conditions, and functional activity is compromised over time [129]. Hence the quality of
264 the resulting biotinylated surface is highly dependent on the experimental conditions.

265 Guo *et al.* [107] also employed NHS ester chemistry, but differently. An aminated
266 surface is firstly carboxylated by treatment with succinic anhydride (Figure 3b). Then,

267 the active ester is formed with a mixture of 1-ethyl-3-(3-dimethylaminopropyl)
268 carbodiimide (EDC) and NHS. Finally, the succinimide ester surface is used to couple
269 amine-containing proteins, such as streptavidin and bovine serum albumin (BSA).

270 Studies carried out in our lab employing the EDC/NHS conjugation of proteins on
271 APTES-modified silicon oxide planar surfaces have shown that the active ester must be
272 formed under well-controlled conditions; for instance, pH must be 3.5. High sensitivity
273 to the experimental conditions implies that this approach lacks reproducibility and
274 provides low yields of protein immobilization. Frequently, the protein remains on the
275 surface after conventional washings due to passive adsorption. Therefore, assessing the
276 covalent attachment of protein acidic washings is recommended.

277 Aminosilane surfaces are also activated with homobifunctional crosslinkers like 1,4-
278 phenylenediisothiocyanate (1,4-PDI), which provide isocyanate groups that react with
279 amine-ended oligonucleotide probes to form a thiourea bond (Figure 3c) [124].
280 However, the most widely used homobifunctional crosslinker is glutaraldehyde (Figure
281 3d), employed to form an aldehyde-terminated surface which allows the reaction of
282 amine groups by the formation of imines (Schiff bases). By this strategy, antibodies,
283 BSA and amine-ended oligonucleotides have been attached to silicon IO devices
284 [63,89,90,108,114]. Due to the reversibility of the imine bond, some authors have
285 reported the use of a sodium cyanoborohydride reduction step to obtain more stable
286 amine bonds [89,108].

287 However, when we attempted this approach on silicon oxide planar surfaces, we
288 observed that when working with a slightly basic pH (9-10), aldolic condensation takes
289 place, providing a short polymer where aminated compounds are covalently attached by
290 single bonds. Thus, reductive conditions are not required to accomplish stable bonds.

291 Another approach which proved robust, reproducible and very suitable for IO
292 biosensors implementation is based on hydrazone bond formation using SoluLink
293 chemistry (Figure 3e) [130,131]. It employs two crosslinkers; 6-hydrazinonicotinamide
294 (S-HyNic) and succinimidyl-4-formylbenzamide (S-4FB); to covalently attach probes
295 on aminated surfaces. This chemistry has been widely used in different configurations
296 for the biofunctionalization of the silicon microring resonators [104,105,132-144]
297 commercialized by Genalyte (to date, the only commercialized device dealing in
298 nanophotonic based biosensing) [145].

299 After accomplishing surface amination with APTMS, 4-polyethylenglycol-4-
300 formylbenzoate (PEG-4FB) is added via succinamide coupling. The probe is previously
301 reacted with a hydrazine nicotinoate (HyNic) moiety by also using succinamide
302 chemistry. Then, a hydrazone bond takes place to covalently link the probe to the
303 surface [132]. The inverse approach can also be used successfully by linking the
304 hydrazine moiety to the surface and modifying the probe with S-4FB [105,133,134].

305 Finally, in order to simplify the number of steps, an organosilane already bearing the
306 HyNic moiety can also be employed to silanize the microring resonator surface
307 [104,135,136,137,138,139,140,141,142,143,144].

308 *SH organosilane*

309 Another approach that also leaves nucleophilic functionality on the surface involves
310 the employment of a thiol-ended organosilane (Figure 4). 3-
311 mercaptopropyltriethoxysilane (MPTS) has been employed by Sepúlveda *et al.* [121]
312 for the functionalization of an integrated Mach-Zehnder interferometer microsystem.
313 This allows a thiolated oligonucleotide to be attached to the surface via disulfide bond
314 linkage (Figure 4a). Thiol functionality also permits the attachment of probes through
315 their amine groups using heterobifunctional crosslinker m-maleimidobenzoyl-N-

316 hydroxysuccinimide ester (MBS), as demonstrated by Xu *et al.* [119] in an
317 implementation of a planar optical waveguide-based interferometer (Figure 4b).

318 The employment of disulfide bonds to attach thiolated oligonucleotides on silanized
319 surfaces offers the advantage of reusability. As the disulfide bond is reversible, the
320 surface can be regenerated, for instance, by treatment with dithiothreitol (DTT).
321 However, this fact has yet to be demonstrated on an IO device.

322 Another interesting approach is that which utilizes the advantageous click chemistry
323 reaction between thiol and alkene moieties (Figure 4c). Our group has demonstrated the
324 biotinylation of silicon oxide surfaces by this principle to perform hybridization assays
325 in a microarray format, which achieves good performance, and is presently being
326 implemented into a ring resonator-based biosensor [146].

327 *Epoxy organosilane*

328 Epoxy chemistry is an alternative coupling system for biomolecule immobilization
329 given its stability under aqueous conditions and its reactivity to several nucleophiles,
330 such as amine and sulfhydryl groups [147,148]. Thus, surfaces that are covalently
331 coated with 3-glycidoxypropyltrimethoxysilane (GOPTS) can be used to conjugate
332 thiol-, amine- or hydroxyl-containing ligands (Figure 5).

333 GOPTS has been employed to covalently attach antibodies and aminated
334 oligonucleotides by an epoxide ring opening in an optical microring resonator by
335 Ramachandran *et al.* (Figure 5a) [113]. Scheneider *et al.* [118] constructed an IO
336 biosensor based on a Hartman interferometer, performed the oxidation of epoxy
337 moieties to aldehyde groups with sodium periodate, and further proved attachment by
338 reductive amination with sodium cyanoborohydride (Figure 5b).

339 In an alternative approach after GOPTS silanization, De Vos *et al.* [101,102] used a
340 thin layer of poly (ethylene) glycol (PEG) to prevent non specific binding in a microring

341 resonator biosensor (avoidance of non specific adsorption is also a critical issue and is
342 dealt with separately). Thus, two heterobifunctional PEGs are used: one bearing thiol
343 and carboxylic acid moieties, and the other containing two amine functionalities, one of
344 them with a protecting group. The use of such reagents allowed the introduction of
345 reactive carboxyl and amino groups onto the surface of the SOI microring. Finally,
346 biotinylation was carried out by EDC/NHS and NH₂-biotin in the first case, and by
347 NHS-biotin in the second [102,110]. Better performance was obtained with the second
348 approach. For the protein attachment on aminated microring resonators,
349 homobifunctional crosslinker di-succinimidyl carbonate (DSC) was also used. However
350 this route proved less efficient than a NHS derivative [101].

351 All the above-mentioned strategies take longer. Recently, we demonstrated the use of
352 epoxy-ended surfaces for the direct attachment of the thiolated oligonucleotides induced
353 by light (Figure 5c). The reaction times are thus cut to a few minutes if compared with
354 the conventional nucleophilic attack of SH [149]. Nucleic acids hybridization assays in
355 the microarray format reveal the potential of this approach which has been employed to
356 develop a microring resonator-based biosensor showing high reproducibility, stability,
357 selectivity and sensitivity to detect hybridized complementary strands with negligible
358 unspecific adsorption (unpublished data).

359 *COOH organosilane*

360 Silane coupling agents containing carboxylate groups have also been utilized to
361 functionalize IO devices with carboxylic acids for the subsequent conjugation with
362 amine-containing molecules (Figure 6a) [58,117]. Duval *et al.* [58] employed
363 carboxyethylsilanetriol sodium salt (CTES) on silicon nitride bimodal waveguide
364 interferometers, and proteins were conjugated to the surface by EDC/NHS. A PhC
365 microcavity sensor was carboxylated by Zlatanovic *et al.* [117] using an effective

366 chelator of metal ions, such as N-(trimethoxysilylpropyl) ethylene-diamine triacetic
367 acid, while proteins were further conjugated by EDC/NHS. After organosilane layer
368 formation, the remaining steps were performed online, and no data on yields or surface
369 characterization are provided, except for the limit of detection for the biorecognition
370 event.

371 In addition, carboxylic acid-ended dimethyl monomethoxy organosilane has been
372 used as a horizontal spacer to form mixed monolayers on a Mach-Zehnder
373 interferometer by the co-adsorption of binary solutions containing both a carboxyl-
374 ended organosilane and another bearing biotin moiety [150]. However, there are no
375 experimental details available on yields, conditions, etc.

376 EDC/NHS-based chemistry for protein conjugation must be carefully carried out
377 because reproducibility is highly dependent on the experimental conditions. Protein
378 attachment to the carboxylated surface can be done in two ways. In a first approach, the
379 active ester is formed on the surface using an acidic pH (3.5), and the protein is
380 conjugated to the surface using a neutral pH (6.5). The second way involves the
381 addition of EDC/NHS together with the protein (pH 6.5), and the conjugation is
382 performed in one step; this case involves the risk of protein cross-conjugation, giving
383 rise to aggregates. Besides in both cases, a risk of hydrolysis of the active ester must be
384 taken into account, and control assays to demonstrate the covalent nature of the link
385 between the protein and the surface are recommended (the protein can remain on the
386 surface through the electrostatic interactions between the amine and the carboxylate
387 moieties, without rendering the advantages of the covalent link).

388 *Isocyanate-ended organosilane*

389 Isocyanatepropyltriethoxysilane (ICPTS) has been used to link proteins onto silicon
390 photonic crystals without crosslinkers or activation steps being needed [106,151]. The

391 isocyanate moiety reacts with amines to form isourea bonds, and with hydroxyl groups
392 to form urethanes (Figure 6b). Oligonucleotides are also attached to the ICPTS surface
393 using biotinylated probes which are affinity-captured by streptavidin covalently linked
394 to the isocyanate modified surface [151]. This is a simple one-step approach, but the
395 experimental conditions must be well-controlled to achieve an acceptable degree of
396 reproducibility. Thus at a certain basic pH, there is a risk of decarboxylation, which
397 provides an amine-ended surface instead of an isocyanate-ended one.

398 It is noteworthy that organosilane-based chemistries are also being successfully
399 applied to other integrated and non integrated optical label-free biosensors developed
400 with different materials, such as glass microspheres [67] and liquid core optofluidic ring
401 resonators [152,153], planar waveguides made of metal oxides, such as Ta₂O₅ [154,155]
402 or SixTi_(1-x)O₂ -as in the commercialized OWLS system based on Optical Waveguide
403 Lightmode Spectroscopy [156]-, and on the TiO₂/SiO₂ surfaces of polymeric PhC
404 [19,157,158] commercialized as BIND™ Biosensor by SRU Biosystems [64].

405 Organosilane condensation on the silicon surface can be done by chemical vapor
406 deposition (CVD) [53,97,100,106,111] or by wet chemistry [111,134]. A good
407 comparison between CVD and wet chemistry was made by Hunt *et al.* [111] for the
408 functionalization of silica microtoroids resonators with APTES, who indicated that
409 chemical vapor deposition provides more ordered monolayers.

410 2.1.2. Other Silicon Surface Chemical Modifications

411 Although silane-based chemistry is the gold standard for the functionalization of
412 silicon-based materials for sensor applications, the literature also describes other
413 alternative surface derivatization approaches for IO biosensors development.

414 Shang *et al.* [159] developed a conjugation strategy based on SAM formation with
415 hydroxyl-ended organophosphonate (Figure 2b) based, in turn, on the “T-BAG” method

416 [160,161]. After SAM formation, divinylsulphone (DVS) was employed as a crosslinker
417 to attach aminated glycanes [162]. Phosphonate chemistry has demonstrated good
418 efficiency in the modification of a Silicon Nanowire-based DNA biosensor [163] and in
419 SAM formation on SiO₂ [164] or Ta₂O₅ [165]. This procedure is also the standard
420 surface modification protocol for the fluorescence microarray chips commercialized by
421 Zeptosens [166,167], made of Ta₂O₅ planar waveguides.

422 Other strategies involve the derivatization of the silicon or silicon nitride by
423 previously removing the native silicon oxide layer. Thus, porous silicon-based devices
424 have been derivatized by hydrosilylation by reacting Si-H bonds with alkene moieties
425 by thermal [168,169] or photochemical activation [170,171]. In this way, carboxylic
426 acid-ended surfaces are obtained and used for aminated probe attaching by EDC/NHS.
427 However, they are yet to be implemented in integrated optics due to long reaction times
428 and the special reaction conditions required. In any case, the employment of
429 photoinduced reactions, involving shorter times and better conditions, is an interesting
430 idea to develop alternative functionalizations for IO devices. Our research group has
431 derivatized silicon nitride with glutaraldehyde through surface N-H bonds after
432 removing the silicon oxide native layer (Figure 2c). This allows the selective attachment
433 of aminated probes against silicon oxide [172]. This approach was used for the
434 biofunctionalization of a highly sensitive silicon nitride slot waveguide microring
435 resonator [173], integrated with microfluidics, to perform excellent sensitivity [174].

436 Finally, other alternative approaches have also been explored by increasing probe
437 loading on the surface while minimizing non specific binding. They are based on the
438 use of dextran hydrogels or dendrimers. [175,176,177]. Thus Goddard *et al.* [175], after
439 a functionalization of a 1D PhC surface with APTMS, used EDC/NHS and a carboxy-
440 terminated dendrimer to attach aminated oligonucleotides (Figure 2f). By utilizing a

441 biotinylated dextran hydrogel, Vollmer *et al.* [177] attached streptavidin-conjugated
442 capture probes onto a silica microsphere cavity biosensor. Dextran-based
443 biofunctionalization has also been applied to IO devices developed on other materials,
444 such as Ta₂O₅ in a Waveguide Interrogated Optical Immunosensor (WIOS) [178].

445 The main biofunctionalization approaches employed to date on IO biosensors are
446 shown in Table S1 (Supplementary Material), and include reaction conditions, type of
447 capture agent and biorecognition event.

448 *2.1.3. Capture Agents Employed as Model Systems*

449 Having performed chemical functionalization on the surface, different capture agents
450 can be attached to the surface: biotin, proteins, antibodies, single-strand nucleic acids,
451 aptamers and carbohydrates.

452 This review classifies biosensors into two groups: those using a model system as
453 proof-of-concept devices and employing capture agents toward targets of analytical
454 interest, and even analyze real samples. The second group is discussed in more detail in
455 Section 3 (Main Achievements).

456 In proof-of-concept IO devices, two main model systems are used: a
457 biotin/streptavidin pair (BT-STV) and a bovine serum albumin/anti bovine serum
458 albumin pair (BSA/anti-BSA). BT-STV is used extensively thanks to its high affinity to
459 recognition and its capacity to display oriented bioreceptors, and it is a well-
460 documented bioaffinity system [53, 97, 100-103,110,111,114,116,118,150].

461 Biotin is used in silicon-based IO biosensors in two ways. First, biotin is the capture
462 agent used to detect streptavidin or avidin, and as a model system to demonstrate the
463 fabricated device's biosensing capability. Thus, avidin biosensing has been seen in IO
464 ring resonators [101,102,110,120], and streptavidin has been used as a target for the
465 biotinylated surfaces of microtoroid resonators [97,100,111], air slot silicon nitride

466 microdisk resonators [114], planar waveguides for Optical Waveguide Lightmode
467 Spectroscopy (OWLS) [103], Mach-Zehnder interferometers [109,150] and ring
468 resonators [116].

469 Second, a biotinylated surface is employed to immobilize a vast variety of biotin-
470 modified probe molecules according to the Avidin-Biotin Complexation (ABC)
471 technique [179,180]. Following this approach, biotinylated Concanavalin A has been
472 immobilized on silicon nitride sensing chips by Reflectometric Interference
473 Spectroscopy [112]. Biotinylated antibodies have also been attached to porous silicon
474 microcavity sensors [88,128], and biotinylated DNA has been employed as a capture
475 agent linked to the surface of a silica microsphere cavity sensor [177].

476 In other devices, streptavidin, covalently attached to the surface, has been used to
477 immobilize the biotinylated capture agent in an oriented fashion in order to perform real
478 sample biosensing [107,108,118,132] (Section 3).

479 The second model system is based on the BSA/anti-BSA (or HSA/anti-HSA) pair.
480 Many studies into biosensing performances have been reported with these systems
481 [84,86,87,102,106,173,174]. This is because BSA adsorbs very well onto the surface
482 and surface functionalization is not absolutely necessary (if surface modification is
483 done, no special care must be taken). BSA is adsorbed on SOI PhC [83,85] and is also
484 covalently immobilized merely to demonstrate protein detection [91], and no further
485 biorecognition event is performed. In other cases, BSA acts as a capture agent to
486 monitor the recognition of its specific antibody (anti-BSA), as in a bimodal waveguide
487 interferometer where BSA is adsorbed [84], and as a photonic crystal waveguide [106]
488 and a slot waveguide ring resonator [173], where BSA is covalently linked to the
489 surface.

490 Other uses of BSA have been presented in the literature. For instance, BSA has been
491 used to carry other moieties responsible for target recognition; e.g., sugars [82] or biotin
492 [117]. Similarly to the BSA/anti-BSA pair, human serum albumin (HSA) and its
493 specific antibody (anti-HSA) have been employed to demonstrate biosensing in silicon
494 nitride Mach-Zehnder interferometers [86,87] and in SOI microring resonators [101].

495 Another pair employed as a model, be it to a lesser extent, is the binding IgG/anti-IgG
496 pair where IgG antibodies are used as capture agents to recognize antiIgG
497 [63,88,109,125,128].

498 When the sensor's capability to detect hybridization events needs demonstrating,
499 oligonucleotide probes can be covalently attached to the surface. Generally, a synthetic
500 fully complementary strand is used to perform hybridization event detection. Such
501 experiments have been carried out on porous silicon-based optical devices [89, 90, 171],
502 silicon nitride-based M-Z Interferometer [121] and SOI-based microring resonators
503 [137,141]. Apart from these, very few examples using receptors other than the
504 aforementioned ones are found in silicon-based IO devices [139,159].

505 After bioreceptor attachment, a blocking step is often performed to avoid non specific
506 binding, which can be achieved in two ways: using a blocking agent after bioreceptor
507 attachment. Thus, BSA has been widely used for this purpose, especially when proteins
508 or antibodies are employed as capture agents [88,107,113,134,135,136]. Commercial
509 blocking buffers like Starting Block [118,137,140,143] PEG [101,115,118] and
510 ovalbumin protein (OVA) have also been employed. Generally in oligonucleotide
511 probes, no blocking step with protein is required, although the chemical blocking of the
512 remaining active sites is necessary. Thus, reducing agents [108] or ethanolamine
513 [58,89,172] are/is used to block aldehyde, isocyanate and epoxy-ended surfaces after
514 bioreceptor attachment. Second, designing surface functionalization chemistry helps

515 avoid biofouling, which is usually done with PEG derivatives [102,112,132] or
516 dendrimers [177].

517 Sometimes, a blocking step is not necessary as non specific binding is negligible
518 [105,133,137]. Non specific binding depends not only on surface modification, but also
519 on the fluidics and buffers employed during biorecognition. Thus, the optimization of
520 such variables can lead to a specific recognition of analytes on unblocked surfaces.

521 Comparing devices is difficult given lack of uniformity when optical biosensor
522 sensitivity is given. So it is not infrequent that the target concentrations needed to
523 distinguish the signal from noise background are very high, but much lower limits of
524 detection from the interpolation in the saturation curve are reported. This is an important
525 issue if the ultimate goal of the device is to act as a real sample biosensor. Table S2
526 (Supplementary Material) presents the sensitivities or limits of detection reported for the
527 IO devices discussed herein, comprising both the lowest target concentration applied to
528 the chip and the reported sensitivity data.

529 *2.2. Techniques Employed for the Biofunctionalization of IO Devices.*

530 From the biofunctionalization viewpoint, one important aspect is to place bioreceptors
531 only in the device's sensing area so that sensitivity remains undiminished. For the time
532 being, this has been accomplished by chemically selective reactions [98,99,172] or by
533 covering the chip with a protecting layer with open windows, but only in the sensing
534 area. This also allows the selective functionalization of each device sensor with the
535 various specific receptors to perform multiplex detection.

536 The receptors are placed in the sensing zone by microspotting –either manually
537 [102,105,133,137] or using a robotic spotter [82,109] – and by employing microfluidics
538 [108,133,134,136,140,143,144]. Despite online functionalization being interesting in
539 the initial stage when setting up and characterizing IO biosensors, it is not the best

540 option if chip fabrication is to be translated to a mass scale. This procedure is time-
541 consuming and presents other problems associated with the microfluidics, such as
542 leaking, channel blocking, cross contamination, etc.

543 *2.3. Characterization Techniques for Modified Surfaces*

544 To check the success of the functionalization process, different characterization
545 techniques are used. Figure 7 provides some examples of characterizations done on IO
546 biosensors. As an initial stage, many researchers use planar substrates to perform the
547 protocol. In general, characterization is accomplished in thickness by ellipsometry
548 [101,109,111,114,172], in hydrophobicity by contact angle measurements
549 [101,171,172], in chemical composition by XPS [98,101,111,115,159,172] and FT-IR
550 spectroscopy [90,92,172], and in topography by AFM [98,115]. Fluorescence
551 microscopy [92,101,114,172,177] and radio labeling [118,181] are also used to assess
552 the bioconjugation of the receptor of interest. However, fluorescence labeling is not
553 suitable when working with silicon surfaces due to this material's quenching effect on
554 tag emission [182]. This fact can be clearly observed in Figure 7a, where a microarray
555 (3x1) of Cy5-labeled goat anti-rabbit antibody (5 ppm in PBS1x) is printed on the
556 surface of Si, silicon nitride and SiO₂ chips respectively, and fluorescence is read with a
557 homemade surface fluorescence reader [183]. As seen, the fluorescence recorded for the
558 silicon surface is considerably lower than that for silicon oxide.

559 However, performances in planar sensors are not necessarily the same as on micro-
560 structured surfaces, and characterization techniques for nanostructures are also required.
561 In general, fluorescence microscopy (Figure 7b) [82,98-100,111,172], SEM (Figure 7c)
562 [97,99,113,172], and TOF-SIMs (Figure 7d) [159] have been used, but their
563 applications are scarce.

564 Another possibility is to use the IO device to monitor the whole functionalization
565 process step by step. For this purpose, microfluidics is used and success in the layer
566 formation is related with the device's RI response [58,104,133,137]. This is an
567 interesting option when the material does not allow the use of fluorescence microscopy
568 and techniques, like the SEM or TOF-SIMS, whose resolution is not sufficient to
569 provide useful information.

570 In conclusion, uniformity and rigor in the systematic characterization of the
571 biofunctionalization process are lacking. In many studies, detection of the target analyte
572 is considered sufficient and no further characterization is performed. In our opinion,
573 knowing the functionalization characteristics allows process modifications that help
574 improve the quality of intermediate layers, which will no doubt affect final biosensor
575 performance.

576

577 **3. Performances and Applications. Main Achievements**

578 This section briefly describes the most interesting advances in IO devices for real
579 sample biosensing. It is worth mentioning that almost all the significant developments
580 made involve targets of clinical interest.

581 The suitability of an optical biosensor for a particular application depends on its
582 performance over a variety of metrics. This includes technical aspects, such as
583 transducer sensitivity and bioassay sensitivity, as well as other parameters that evaluate
584 market success possibilities (ease-of-use, sensor cost, portability, scalability and
585 throughput).

586 Transducer sensitivity is defined as variation in either the sensor output response
587 resulting from a unit change refractive index (denominated bulk sensitivity) or the mass
588 density (called surface sensitivity) on the sensor surface. It is independent of a

589 biofunctionalization process being performed and is used for sensor characterization at a
590 basic level. However, the bioassay sensitivity must be measured to evaluate the device's
591 real biosensing capability and is the response variation to a given change in analyte
592 concentration. It depends on both the biofunctionalization process and the affinity
593 constant between receptor and analyte. Thus when working with the same optical
594 device, high-molecular-weight molecules with a high affinity to the receptor are
595 detected at lower concentrations than small molecules with a low binding affinity. It
596 should be noted that the assay sensitivity value is mandatory if real biosensing is
597 claimed.

598 Table 1 summarizes the most relevant results obtained to date in real sample
599 biosensing using IO devices.

600 One platform demonstrating good performance for real sample biosensing is SOI
601 microring resonators. Different assays have been performed in them using the
602 hydrazine/aldehyde conjugation chemistry. By employing aminated DNA
603 oligonucleotide probes attached to the surface, closely related bacterial species (*S.*
604 *neumoniae* and *S. agalacticae*) are distinguished by monitoring specific probe
605 hybridization with microRNAs (mRNAs) in a single, multiplexed assay; the smallest
606 mRNA amount detected is 53 fmol [105]. This method has proven reproducible, and
607 dehybridization with RNase enzyme enables sensor surface regeneration [133].
608 Sensitivity is improved by amplification using anti-DNA:RNA antibodies and by
609 lowering the detected concentration to 350 amol (10 pM). With this device, the
610 isothermal discrimination of DNA single nucleotide polymorphisms (SNPs) is achieved
611 [137], and DNA-encoded antibodies against prostate specific antigen (PSA) and α -
612 fetoprotein (AFP) are used to demonstrate the multiplex screening of capture agent
613 binding properties [138,143]. The DNA encoding strategy consists in a self-assembly

614 process where antibodies are previously conjugated to specific sequences that are
615 complementary to the DNA strands immobilized on the surface. It has an advantage
616 over direct antibody covalent immobilization, that of improving its binding capacity (as
617 it is oriented). Surface regeneration by a dehybridization step is also possible.
618 Antibodies are also covalently attached to the surface to perform quantitative,
619 multiplexed analyses of clinically relevant protein biomarkers: PSA, AFP,
620 carcinoembryonic antigen (CEA), tumor necrosis factor- α (TNF- α) and interleukin-8
621 (IL-8) by direct immunoassays [134,144]. Covalently linked antibodies are also used for
622 the quantitation of biomarker C-reactive protein (CRP) in human serum and plasma
623 directly and by a sandwich immunoassay, followed by a bead-enhanced third binding
624 event to increase sensitivity [142]. Other interesting applications of such IO devices
625 include: the specific, quantitative, multiplexed cytokine analysis of T-cell secretion by a
626 one-step sandwich immunoassay [136,140], the multiplex binding kinetics
627 determination of thrombin-binding DNA aptamer and anti-thrombin monoclonal
628 antibody [139], or the quantitative detection of *Bean pod mottle virus* from leaf samples
629 by direct immunoassay, involving quicker sample preparation and with a limit of
630 detection of 10 ng mL^{-1} [135]. Carbohydrate-protein and norovirus particle interactions
631 are characterized by the same microring resonator sensor array and organophosphonate
632 based chemistry [159]. However, the results reported when this approach was adopted
633 are preliminary, and the established and widely demonstrated methodology to
634 functionalize microring resonators is that based on hydrazine-aldehyde conjugation.

635 Vertically coupled high refractive index microring resonators show the specific
636 capture of whole bacteria cell *E. coli* O157:H7 by direct immunoassay after the covalent
637 immobilization of the specific monoclonal antibody using GOPTS [113]. Although

638 control assays do not reveal the covalent nature of antibody attachment in this case,
639 bacteria recognition proves specific.

640 By utilizing an integrated innovative bimodal waveguide interferometer, Duval *et al.*
641 [58] recently demonstrated the picomolar detection level of human hormone hTSH by
642 an indirect competitive immunoassay. In this case, carboxy-ended organosilane is used
643 to functionalize the surface; while the hormone (antigen) is attached to the sensor
644 through amine groups using EDC/NHS (no details of surface chemistry and
645 characterization are provided). The specific antibody to hTSH is recognized by the
646 receptor on the surface in an inversely proportional manner to the amount of hormone
647 present in the sample. These methods are sensitive (20 pM), reproducible and specific.

648 With a Mach-Zehnder interferometer design with planar optical waveguides, Xu *et al.*
649 [119] also specifically recognized three avian influenza virus subtypes by direct
650 immunoassay, with limits of detection of $5 \cdot 10^{-4}$ hemagglutination units per milliliter
651 (HA units mL⁻¹). In this case, SH-ended organosilane is used and specific antibodies are
652 attached to the surface by a 1-hour incubation with m-Maleimidobenzoyl-N-
653 hydroxysuccinimide ester as the crosslinker. Stability under storage at 4 °C for several
654 days is demonstrated.

655 Ymeti *et al.* [56] used a four-channel integrated Young interferometer for the
656 detection of herpes simplex virus type 1 (HSV-1) by a direct immunoassay with
657 monoclonal specific antibodies immobilized on the surface via protein A in an oriented
658 fashion. The whole process is developed online by monitoring real-time surface
659 changes. Two points of this demonstrator must be highlighted; first, the specificity of
660 the recognition is assessed by immobilizing different receptor layers in adjacent
661 measuring channels and by monitoring the sensor response to different analyte
662 solutions. Second, although protein A is adsorbed on the surface, negligible desorption

663 is noted for the analysis time, as observed from the baseline. Finally, solutions are
664 allowed to flow over the sensor for no longer than 30 min, and very good results are
665 obtained. Sensitivity is very high ($850 \text{ particles mL}^{-1}$) and the blood serum analysis is
666 also reported, be it with lower sensitivity [81].

667 Antibodies covalently attached on the surface of a Hartman interferometer-based
668 optical chip have been reported by Schneider *et al.* [118] to detect human chorionic
669 gonadotropin (hCG) in serum and whole blood. For this purpose, a sandwich
670 immunoassay is performed using gold labeled secondary antibody to increase sensitivity
671 (0.1 ng mL^{-1}). Chemical surface functionalization is accomplished by silanization with
672 GOPTS, followed by oxidative epoxy ring opening to provide an aldehydized surface.
673 Then, avidin is attached to the surface by reductive amination and biotinylated-specific
674 antibodies are bound to this surface. However, the most interesting point of this work is
675 the study into non specific binding during measurements and how to compensate it
676 using a reference channel.

677 Qiao *et al.* [169] have demonstrated the first implementation of a porous silicon-based
678 Bloch surface sensor for protease activity detection ($7 \mu\text{g mL}^{-1}$) based on the digestion
679 of gelatin covalently attached to the surface. In this case, a hydrosilylation process is
680 employed as the first modification step. This approach comprises many further steps,
681 but sensitivity is poor; thus, it is not so interesting.

682 Armani *et al.* [184] have employed silicon-based microtoroids resonators to
683 demonstrate real biosensing with extremely low sensitivities. To that end, protein G is
684 adsorbed on the surface to bind by affinity-specific antibodies and to detect IL-2 in fetal
685 bovine serum with a sensitivity close to a single molecule ($5 \cdot 10^{-18} \text{ M}$). PhC-based
686 sensors have also demonstrated the capability of real biosensing. The so-called
687 nanoscale optofluidic sensor array (NOSA) [185] has been used for the multiplex

688 detection of three interleukins (IL-4, IL-6, IL-8) by sandwich immunoassays.
689 Streptavidin is covalently attached to the surface by using APTES and glutaraldehyde,
690 which allow the oriented immobilization of biotinylated capture antibodies. Despite
691 sensitivity not being that good ($1 \mu\text{g mL}^{-1}$), it is one of the first demonstrations of real
692 multiplex biosensing with PhC [108]. With the same device and by also employing
693 APTES and glutaraldehyde, four serotypes of Dengue virus were detected by
694 immobilizing four specific DNA oligonucleotides and performing hybridization after
695 adding the specific targets to the sensor [186].

696 As seen, the sensor biofunctionalization conditions employed are diverse and vary in
697 terms of assay times, blocking process, etc. To date, the most extensive, characterized
698 work is that developed with microring resonators using hydrazine-aldehyde chemistry.
699 A comparative study which adopts different approaches for the same sensor design and
700 for the same bioassay is still lacking, along with any advances made in this research
701 field.

702

703 **4. Future Trends**

704 One of the main advantages of IO technology is the possibility to integrate all
705 functions (chemistry, optics, fluidics and electronics) into a single platform. Despite
706 significant advances having been made in recent years toward developing IO biosensors
707 capable of acting as point-of-care or lab-on-a-chip devices, several issues remain to be
708 explored. The choice of the surface modification, biofunctionalization procedures, and
709 the detection assay type and conditions, become a relevant issue to consider, together
710 with the development and optimization of integrated optics-based sensing structures.
711 Some interesting aspects to be studied in the future, which have the potential to improve
712 already existing performance, are discussed in this section.

713 The effective and selective patterning for spatial control in the biofunctionalization of
714 sensors to help accomplish high-density multiplexing has not yet been fully achieved.
715 The use of automatic printers or microfluidic systems is a good option, but both
716 techniques are quite time-consuming, and the search for easier and faster alternatives is
717 an objective. In this sense, photoactivated coupling reactions, especially those in the
718 click-chemistry group, have demonstrated their utility in planar platforms [146,187] and
719 can be an interesting possibility to explore their application in the multiplex
720 biofunctionalization of high-density array sensors.

721 Moreover, new conjugation techniques that simplify the number of steps and place
722 capture agents close to the surface in a bioavailable manner, while providing a robust
723 and reproducible link, are another unexploited field of study. The analyses of next-
724 generation capture agents that improve the performance of those already in use are also
725 desirable.

726 Designing approaches that allow surface regeneration and provide versatility, as in the
727 DNA-encoding strategy, should be one of the preferred options for new developments.
728 There is a large number of novelties in relation to capture agents for real biosensing to
729 be explored in the IO devices whose efficiency has been demonstrated on other assay
730 platforms, such as the triplex affinity capture methods or use of synthetic (aptamers) or
731 semi-synthetic molecules (peptide nucleic acids, PNA) as new probes [188-191].

732 Another highly desirable option is to find biofunctionalization strategies that are
733 compatible with the manufacturing process of devices. This would make them mass
734 production scalable, and would help them reach truly applicable point-of-need devices
735 ready for end users.

736 Finally, the establishment of a testing model system would facilitate the comparison
737 between devices. This system should include not only checking on specific binding, but
738 also stability tests of functionalized devices for long-term storage.

739 The issues discussed above rely only on the chemical functionalization of the surface
740 and anchoring of bioreceptors.

741 However, it is noteworthy that these developments have to be coupled with advances
742 in other fields such as optics, fluidics and electronics. It is only in this way that real
743 progress in the vast, multidisciplinary task of managing to manufacture RI integrated
744 optical devices capable of providing fast, specific and sensitive responses at the point of
745 need will be feasible.

746

747 **Acknowledgements**

748 This research has been supported by the Spanish Ministry of Science and Innovation
749 through project CTQ2010-15943/BQU and by the Regional Valencian Government,
750 through GVA/PROMETEO 2010/08. The authors thank Dr. Miguel Holgado, from the
751 Universidad Politécnica de Madrid, for his helpful discussion about the classification of
752 RI optical sensors.

753

754

- 756 [1] W.E. Moerner, *Proc. Natl. Acad. Sci.* 104 (2007) 12596-12602.
- 757 [2] Y.S. Sun, J.P. Landry, Y.Y. Fei, X.D. Zhu, J.T. Luo, X.B. Wang, K.S. Lam,
758 *Langmuir* 24, (2008) 13399-13405.
- 759 [3] M.A. Cooper, *Label-Free Biosensors: Techniques and Applications*,
760 Cambridge University Press, NY, USA, 2009.
- 761 [4] A.K. Shiau, M.E. Massari, C.C. Ozbil, *Combinatorial Chem. High*
762 *Throughput Screen.* 11 (2008) 231-237.
- 763 [5] A.J. Qavi, A.L. Washburn, J.-Y. Byeon, R.C. Bailey, *Anal Bioanal. Chem.*
764 394 (2009) 121-135
- 765 [6] H.K. Hunt, A.M. Armani, *Nanoscale* 2 (2010) 1544-1559.
- 766 [7] C. Monat, P. Domachuck, *Nature Photon.* 1 (2007) 106-114.
- 767 [8] D.W. Kimmel, G. LeBlanc, M.E. Meschievitz, D.E. Cliffel, *Anal. Chem.* 84
768 (2012), 685-707.
- 769 [9] Q. Xiang, Y. Gao, J. Liu, K. Wang, J. Tang, M. Yang, S. Wang, W. Wang,
770 *Adv. Mater. Res.* (2012) 418-420.
- 771 [10] F. Berti, A.P.F. Turner, *Biosensor Nanomaterials* (2011) 1-35.
- 772 [11] D. Grieshaber, R. MacKenzie, J. Voros, E. Reimhult, *Sensors* 8 (2008) 1400-
773 1458.
- 774 [12] A. Matsumoto, Y. Miyahara, *Drug Delivery System* 26 (2011) 15-19.
- 775 [13] B. Lindholm-Sethson, J. Nystroem, M. Malmsten, L. Ringstad, A. Nelson, P.
776 Geladi, *Anal. Bioanal Chem.* 398 (2010) 2341-2349.
- 777 [14] G.N.M. Ferreira, A.C. da-Silva, B. Tome, *Trends in Biotechnology* 27 (2009)
778 689-697.
- 779 [15] M. Alvarez, L.M. Lechuga, *Analyst* 135 (2010) 827-836.
- 780 [16] M. Álvarez, L.G. Carrascosa, K. Zinoviev, J.A. Plaza, L.M. Lechuga, in:
781 *Biosensors and Biodetection. Methods and Protocols*, Vol 2, Series: Methods
782 in Molecular Biology, Vol. 504, Humana Press, Springer, 2009.
- 783 [17] K. Gruber, T. Horlacher, R. Castelli, A. Mader, P.H. Seeberger, B.A.
784 Hermann, *ACS Nano* 5 (2011) 3670-3678.
- 785 [18] J.L. Arlett, E.B. Myers, M.L. Roukes, *Nat. Nanotechnol.* 6 (2011) 203-215.
- 786 [19] S. George, I.D. Block, S.I. Jones, P.C. Mathias, V. Chaudhery, P.
787 Vuttipittayamongkol, H.-Y. Wu, L.O. Vodkin, B.T. Cunningham, *Anal.*
788 *Chem.* 82 (2010) 8551-8557.
- 789 [20] V. Velusamy, K. Arshak, O. Korostynska, K. Oliwia, C. Adley, *Biotechnol.*
790 *Adv.* 28 (2010) 232-254.
- 791 [21] O. Lazcka, F.J. del Campo, F.X. Muñoz, *Biosens. Bioelectron.* 22 (2007)
792 1205-1217.
- 793 [22] H.M. Haake, A. Schutz, G. Gauglitz, *Fresenius J. Anal. Chem.* 366 (2000)
794 576-585.
- 795 [23] G. Gauglitz, G. Proll, *Adv. Biochem. Engin./Biotechnol.* 109 (2008) 395-432.
- 796 [24] F. Proell, P. Fechner, G. Proll, *Anal. Bioanal. Chem.* 393 (2009) 1557-1562.
- 797 [25] X. Fan, I.M. White, S.I. Shopova, H. Zhu, J.D. Suter, Y. Sun, *Anal. Chim.*
798 *Acta* 620 (2008) 8-26.
- 799 [26] M.M. Mariani, P.J.R. Day, V. Deckert, *Integrative Biology* 2 (2010) 94-101.
- 800 [27] I. Notingher, *Sensors* 7 (2007) 1343-1358.
- 801 [28] S.E. Lee, L.P. Lee, *Curr. Opin. Biotechnol.* 21 (2010) 489-497.
- 802 [29] B. Yan, S.V. Boriskina, B.M. Reinhard, *J. Phys. Chem.* 115 (2011) 24437-
803 24453.

- 804 [30] W. Xie, L. Su, A. Shen, A. Materny, J. Hu, *J. Raman Spectrosc.* 42 (2011)
805 1248-1254.
- 806 [31] J. Breault-Turcot, J.-F. Masson, *Anal. Bioanal. Chem.* 403 (2012) 1477-
807 1484.
- 808
- 809 [32] A. Shalabney, I. Abdulhalim, *Laser Photonics Rev.* 5 (2011) 571-606.
- 810 [33] H.W. Choi, Y. Sakata, Y. Kurihara, T. Ooya, T. Takeuchi, *Anal. Chim. Acta*
811 728 (2012) 64-68.
- 812 [34] T. Kumeria, M.D. Kurkuri, K.R. Diener, L. Parkinson, D. Losic, *Biosens.*
813 *Bioelectron.* 35 (2012) 167-173.
- 814 [35] B.J. Cowsill, T.A. Waigh, S. Eapen, R. Davies, J.R. Lu, *Soft Matter* 8 (2012)
815 9847-9854.
- 816 [36] Y. Wang, J. Wang, F. Yang, X. Yang, *Anal. Chem.* 84 (2012) 924-930.
- 817 [37] B.T. Cunningham, *JALA* 15 (2010) 120-135.
- 818 [38] S.M. Shama, B.T. Cunningham, *Analyst* 136 (2011) 1090-1102.
- 819 [39] M.S. Luchansky, R.C. Bailey, *Anal. Chem.* 84 (2012), 793-821.
- 820 [40] A.M. Armani, in: I. Chemros, N. Uzunoglu, O. Schwelb. (Eds.), *Photonic*
821 *Microresonators Research and Applications*, Springer Series in optical
822 *Sciences*, Springer-Verlag New York Inc. 2010, pp. 253-273.
- 823 [41] M.C. Estevez, M. Alvarez, L.M. Lechuga, *Laser Photonics Rev.* 6 (2011)
824 463-487.
- 825 [42] V. Gubala, L.F. Harris, A.J. Ricco, M.X. Tang, D.E. Williams, *Anal. Chem.*
826 84 (2012) 487-515.
- 827 [43] F.S. Liegler, *Anal. Chem.* 81 (2009) 519-526.
- 828 [44] A.L. Washburn, R.C. Bailey, *Analyst* 136 (2011) 227-236.
- 829 [45] L.F. Capitan-Vallvey, A.J. Palma, *Anal. Chim. Acta* 696 (2011) 27-46.
- 830 [46] A. Kussrow, C.S. Enders, D.J. Bornhop, *Anal. Chem.* 84 (2012) 779-792.
- 831 [47] J. Vörös, J.J. Ramsden, G. Csúcs, I. Szendro, S.M.D. Paul, M. Textor, N.D.
832 Spencer, *Biomater.* 23 (2002) 3699-3710.
- 833 [48] K. Schmitt, K. Oehse, G. Sulz, C. Hoffmann, *Sensors* 8 (2008) 711-738.
- 834 [49] H. Zhu, J. D. Suter, X. Fan, in: *Optical guided-Wave Chemical and*
835 *Biosensors II*, Springer Series on Chemical Sensors and Biosensors 8 (2010)
836 259-279.
- 837 [50] H. Sohlström, K.B. Gylfason, D. Hill, *proc. SPIE* 7719 (2010) 1-15.
- 838 [51] Y. Sun, X. Fan, *Anal. Bioanal. Chem.* 399 (2011) 205-211.
- 839 [52] J. Ward, O. Benson, *Laser Photonics Rev.* 5 (2011) 553-570.
- 840 [53] A. Densmore, M. Vachon, D.X. Xu, S. Janz, R. Ma, Y.H. Li, G. Lopinsly, A.
841 Delange, J. Lapointe, C.C. Leubbert, Q.Y. Liu, P. Cheben, J.H. Schmid, *Opt.*
842 *Lett.* 34 (2009) 3598-3600.
- 843 [54] K. Zinoviev, L.G. Carrascosa, J. Sánchez del Río, B. Sepúlveda, C.
844 Domínguez, L.M. Lechuga, *Adv. Opt. Technol.* Article ID 383927 (2008) 1-
845 6.
- 846 [55] A. Crespi, Y. Gu, B. Ngamsom, H.J.W. Hoekstra, C. Dongre, M. Pollnau, R.
847 Ramponi, H.H. van den Vlekkert, P. Watts, G. Cerullo, R. Osellame, *Lab*
848 *Chip* 10 (2010) 1167-1173.
- 849 [56] A. Ymeti, J. Greeve, P.V. Lambeck, R. Wijn, R.G. Heideman, J.S. Kanger,
850 *Appl. Opt.* 44 (2005) 3409-3412.
- 851 [57] K. Schmitt, B. Schirmer, C. Hoffmann, A. Brandenburg, P. Meyrueis,
852 *Biosens. Bioelectron.* 22 (2007) 2591-2597.

- 853 [58] D. Duval, A.B. González-Guerrero, S. Dante, J. Osmond, R. Monge, L.J.
854 Fernández, K. E. Zinoviev, C. Domínguez, L.M. Lechuga, *Lab Chip* 12
855 (2012) 1987-1994.
- 856 [59] M. Holgado, C.A. Barrios, F.J. Ortega, F.J. Sanza, R. Casquel, M.F. Laguna,
857 M.J. Bañuls, D. Lopez-Romero, R. Puchades, A. Maquieira, *Biosens.*
858 *Bioelectron.* 25 (2010) 2553-2558.
- 859 [60] F.J. Sanza, M. Holgado, F.J. Ortega, R. Casquel, D. López-Romero, M.J.
860 Bañuls, M.F. Laguna, C.A. Barrios, R. Puchades, A. Maquieira, *Biosens.*
861 *Bioelectron.* 26 (2011) 4842-4847.
- 862 [61] J. Adrian, S. Pasche, D.G. Pinacho, H. Font, J.M. Diserens, F. Sánchez-
863 Baeza, B. Granier, G. Voirin, M.-P. Marco, *Trends Anal. Chem.* 28 (2009)
864 769-777.
- 865 [62] C. Monat, P. Domachuk, B.J. Eggleton, *Natt. Photonics* 1 (2007) 106-114.
- 866 [63] S. Pal, E. Guilermain, R. Sriram, B.L. Miller, P.M. Fauchet, *Biosens.*
867 *Bioelectron.* 26 (2011) 4024-4031.
- 868 [64] www.srubiosystems.com
- 869 [65] F. Vollmer, S. Arnold, *Nat. Methods* 5 (2008) 591-596.
- 870 [66] H.A. Huckabay, R.C. Dunn, *Sens. Actuators B* 160 (2011) 1262-1267.
- 871 [67] K.A. Wilson, C.A. Finch, P. Anderson, F. Vollmer, J.J. Hickman, *Biometr.*
872 33 (2012) 225-236.
- 873 [68] I.M. White, H. Zhu, J.D. Suter, X. Fan, M. Zourob, in: A. Rasooly K. E:
874 Herold (Eds.), *Methods in Molecular Biology: Biosensors and Biodetection*
875 503, Humana Press, 2009, pp 139-165.
- 876 [69] O.S. Wolfbeis, *Anal. Chem.* 80 (2008) 4269-4283.
- 877 [70] H. Gai, Y. Li, E.S. Yeung, *Top. Curr. Chem.* 304 (2011) 107-201.
- 878 [71] F.B. Myers, L.P. Lee, *Lab Chip* 8 (2008) 2015-2031.
- 879 [72] X. Fan, I.M. White, *Nat. Photonics* 5 (2011) 591-597.
- 880 [73] D.K. Aswal, S. Lenfant, D. Guerin, J.V. Yakhami, D. Villaume, *Anal. Chim.*
881 *Acta* 568 (2006) 84-108.
- 882 [74] M. Stutzmann, J. A. Garrido, M. Eickhoff, M. S. Brandt, *Phys. Status Solidi*
883 *A* 203 (2006) 3424-3437.
- 884 [75] R.J. Hamers, *Annu. Rev. Anal. Chem.* 1 (2008) 707-736.
- 885 [76] J.N. Chazalviel, P. Allongue, A.C. Gouget-Laemmel, C. Henry de
886 Villeneuve, A. Moraillon, F. Ozanam, *Sci. Adv. Mater.* 3 (2011) 332-353.
- 887 [77] E. Sudholter, L.C.P.M. De Smet, M. Mescher, D. Uliien, in: A. Hashim (Ed.),
888 *Nanowires-Implementations and Applications* (2011) pp 267-288.
- 889 [78] G. Collins, J.D. Holmes, *J. Mater. Chem.* 21 (2011) 11052-11069.
- 890 [79] A. Ymeti, J.S. Kanger, J. Greve, G.A.J. Besselink, P.V. Lambeck, R. Wijn,
891 R.G. Heideman, *Biosens. Bioelectron.* 20 (2005) 1417-1421.
- 892 [80] L.M. Freeman, S. Li, Y. Dayani, H.-S. Choi, N. Malmstadt, A.M. Armani,
893 *Appl. Phys. Lett.* 98 (2011) 143703-1-3.
- 894 [81] A. Ymeti, J. Greve. P.V. Lambeck, T. Wink, S.W.F.M. van Hövell, T.A.M.
895 Beumer, R.R. Wijn, R.G. Heideman, V. Subramaniam, J.S. Kanger, *Nano.*
896 *Lett.* 7 (2007) 394-307.
- 897 [82] J.T. Kirk, G.E. Friedly, J.W. Chamberlain, E.D. Christensen, M. Hochberg,
898 D.M. Ratner, *Lab Chip* 11 (2011) 1372-1377.
- 899 [83] D. Dorfner, T. Zabel, T. Hürlimann, N. Hauke, L. Frandsen, U. Rant, G.
900 Abstreiter, J. Finley, *Bioens. Bioelectron.* 24 (2009) 3688-3692.
- 901 [84] K.E. Zinoviev, A.B. González-Guerrero, C. Domínguez, L.M. Lechuga, J.
902 *Lightwave Technol.* 29 (2011) 1926-1930.

- 903 [85] N. Skivesen, A. Têtu, M. Kristensen, J. Kjems, L.H. Frandsen, P.I. Borel,
904 Opt. Express 15 (2007) 3169-3176.
- 905 [86] F. Prieto, B. Sepúlveda, A. Calle, A. Llobera, C. Domínguez, L.M. Lechuga,
906 Sens. Actuators B 92 (2003) 151-158.
- 907 [87] F. Prieto, L.M. Lechuga, A. Calle, A. Llobera, C. Domínguez, J. Lightwave
908 Technol. 19 (2001) 75-83.
- 909 [88] L.M. Bonanno, L.A. DeLouise, Biosens. Bioelectron. 23 (2007) 444-448.
- 910 [89] G. Rong, A. Najmaie, J.E. Sipe, S.M. Weiss, Biosens. Bioelectron. 23 (2008)
911 1572-1576.
- 912 [90] De Tommasi, L. De Stefano, I. Rea, V. Di Sarno, L. Rotiroti, P. Arcari, A.
913 Lamberti, C. Sanges, I. Rendina, Sensors 8 (2008) 6549-6556.
- 914 [91] M. Lee, P.M. Fauchet, Opt. Express 15 (2007) 4530-4535.
- 915 [92] N. Massad-Ivanir, G. Shtenberg, A. Tzur, M.A. Krepker, E. Segal, Anal.
916 Chem. 83 (2011) 3282-3289.
- 917 [93] A. Ulman, Chem. Rev. 96 (1996) 1533-1554.
- 918 [94] S. Onclin, B. J. Ravoo, D.N. Reinhoudt, Angew. Chem. Int. Ed. 44 (2005)
919 6282-6304.
- 920 [95] D. Wouters, S. Hoepfener, J.P.E. Sturms, U.S. Schubert, J. Scann. Probe
921 Microsc. 1 (2006) 45-50.
- 922 [96] J.A. Howarter, J.P. Youngblood, Langmuir 22 (2006) 11142-11147.
- 923 [97] C. Shi, S. Mehrabani, A.M. Armani, Opt. Lett. 37 (2012) 1643-1645.
- 924 [98] B.W. Biggs, H.K. Hunt, A.M. Armani, J. Colloid Interface Sci. 369 (2012)
925 477-481.
- 926 [99] H.K. Hunt, A.M. Armani, Opt. Lett. 36 (2011) 1092-1094.
- 927 [100] C.E. Soteropoulos, H.K. Hunt, A.M. Armani, Appl. Phys. Lett. 99 (2011)
928 103703-1-3.
- 929 [101] K. De Vos, J. Girones, T. Claes, S. Popelka, E. Schacht, R. Baets, P.
930 Bienstman, IEEE Photonics J. 1 (2009) 225-235.
- 931 [102] De Vos, J. Girones, S. Popelka, E. Schacht, R. Baets, P. Bienstman, Biosens.
932 Bioelectron. 24 (2009) 2528-2533.
- 933 [103] S. Grego, J.R. McDaniel, B.R. Stoner, Sens. Actuators B 131 (2008) 347-355.
- 934 [104] J.-Y. Byeon, F.T. Limpoco, R.C. Bailey, Langmuir 26 (2010) 15430-15435.
- 935 [105] O. Scheler, J.T. Kindt, A.J. Qavi, L. Kaplinski, B. Glynn, T. Barry, A. Kurg,
936 R.C. Bailey, Biosens. Bioelectron. 36 (2012) 56-61.
- 937 [106] J. García-Rupérez, V. Toccafondo, M.J. Bañuls, J. García Castelló, A. Griol,
938 S. Peransí-Llopis, A. Maquieira, Opt. Express 18 (2010) 24276-24286.
- 939 [107] Y. Guo, J.Y. Ye, C. Divin, B. Huang, T.P. Thomas, J.R. Baker, T.B. Norris,
940 Anal. Chem. 82 (2010) 5211-5218.
- 941 [108] S. Mandal, J.M. Goddard, D. Erickson, Lab Chip 9 (2009) 2924-2932.
- 942 [109] A. Densmore, D.-X. Xu, S. Janz, P. Waldron, T. Mischki, G. Lopinski, A.
943 Delâge, J. Lapointe, P. Cheben, B. Lamontagne, J.H. Schmid, Opt. Lett. 33
944 (2008) 596-598.
- 945 [110] De Vos, I. Bartolozzi, E. Schacht, P. Bienstman, Opt. Express 15 (2007)
946 7610-7615.
- 947 [111] H.K. Hunt, C. Soteropolos, A.M. Armani, Sensors 10 (2010) 9317-9336.
- 948 [112] H.-W. Choi, H. Takahashi, T. Ooya, T. Takeuchi, Anal. Methods 3 (2011)
949 1366-1370.
- 950 [113] A. Ramachandran, S. Wang, J. Clarke, S.J. Ja, D. Goad, L. Wald, E.M. Flood,
951 E. Knobbe, J.V. Hryniewicz, S.T. Chu, D. Gill, W. Chen, O. King, B.E.
952 Little, Biosens. Bioelectron. 23 (2008) 939-944.

- 953 [114] S. Lee, S.C. Eom, J.S. Chang, C. Huh, G.Y. Sung, J.H. Shin, *Opt. Express* 18
954 (2010) 20638-20644.
- 955 [115] S. Sharma, R.W. Johnson, T.A. Desai, *Biosens. Bioelectron.* 20 (2004) 27-
956 239.
- 957 [116] A. Densmore, D.-X. Xu, S. Janz, P. Waldron, J. Lapointe, T. Mischki, G.
958 Lopinski, A. Delâge, J.H. Schmid, P. Cheben, *Adv. Opt. Technol.* (2008) ID
959 755967.
- 960 [117] S. Zlatanovic, L.W. Mirkarimi, M.M. Sigalas, M.A. Bynum, E. Chow, K.M.
961 Robotti, G.W. Burr, S. Esenar, A. Grot, *Sens. Actuators B* 141 (2009) 13-19.
- 962 [118] B.H. Schneider, E.L. Dickinson, M.D. Vach, J.V. Hoijer, L.V. Howard,
963 *Biosens. Bioelectron.* 15 (2000) 13.-22.
- 964 [119] J. Xu, D. Suarez, D.S. Gottfried, *Anal. Bioanal. Chem.* 389 (2007) 1193-
965 1199.
- 966 [120] A. Ksendzov, Y. Lin, *Opt. Lett.* 30 (2005) 3344-3346.
- 967 [121] B. Sepúlveda, J. Sánchez del Río, M. Moreno, F.J. Blanco, K. Mayora, L.M.
968 Lechuga, *J. Opt. A: Pure Appl. Opt.* 8 (2006) S561-S566.
- 969 [122] C. Haensch, S. Hoeppeener, U.S. Schubert, *Chem. Soc. Rev.* 39 (2010) 2323-
970 2334.
- 971 [123] G.T. Hermanson, in *Bioconjugate Techniques*, 2nd Ed Academic Press:
972 London, UK, 2008, pp 562-581.
- 973 [124] Z.B. Bahsi, A. Büyükkaksoy, S.M. Ölmezcan, F. Simsek, M.H. Aslan, A.Y.
974 Oral, *Sensors* 9 (2009) 4890-4900.
- 975 [125] D.-X. Xu, M. Vachon, A. Densmore, R. Ma, S. Janz, A. Delâge, J. Lapointe,
976 P. Cheben, J. H. Schmid, E. Post, S. Messaoudène, J.-M. Fédéli, *Opt. Express*
977 18 (2010) 22867-22879.
- 978 [126] E.T. Vanderberg, L. Bertilsson, B. Liedberg, K. Uvdal, R. Erlandson, H.
979 Elwing, *I. Lundstrom, J. Colloid Interface Sci.* 147 (1991) 103-118.
- 980 [127] D.-X. Xu, M. Vachon, A. Densmore, R. Ma, A. Delâge, S. Janz, J. Lapointe,
981 Y. Li, G. Lopinski, D. Zhang, Q.Y. Liu, P. Cheben, J.H. Schmid, *Opt. Lett.*
982 35 (2010) 2771-2773.
- 983 [128] L.M. Bonanno, L.A. DeLouise, *Langmuir* 23 (2007) 5817-5823.
- 984 [129] S.Y. Wong, D. Putnam, *Bioconjugate Chem.* 18 (2007) 970-982.
- 985 [130] R. Greenfield, T. Taneko, A. Daues, M. Edson, K. Fitzgerald, L. Olech, J.
986 Grattan, G. Braslawsky, *Cancer Res.* 50 (1990) 6600-6607.
- 987 [131] <http://www.solulink.com/>
- 988 [132] M. Iqbal, M.A. Gleeson, B. Spaugh, F. Tybor, W.G. Gunn, M. Hochberg, T.
989 Baehr-Jones, R.C. Bailey, C. Gunn, *IEEE J. Selected Topic in Quantum*
990 *Electronics* 16 (2010) 654-661.
- 991 [133] A.J. Qavi, R.C. Bailey, *Angew. Chem. Int. Ed.* 49 (2010) 4608-4611.
- 992 [134] A.L. Washburn, L.C. Gunn, R.C. Bailey, *Anal. Chem.* 81 (2009) 9499-9506.
- 993 [135] M.S. Clellan, L.L. Domier, R.C. Bailey, *Biosens. Bioelectron.* 31 (2012) 388-
994 392.
- 995 [136] M.S. Luchansky, R.C. Bailey, *Anal. Chem.* 82 (2010) 1975-1981.
- 996 [137] A. Qavi, T.M. Mysz, R.C. Bailey, *Anal. Chem.* 83 (2011) 6827-6833.
- 997 [138] M.T. Marty, C.D.K. Sloan, R.C. Bailey, S.G. Sligar, *Anal. Chem.* 84 (2012)
998 5556-5564.
- 999 [139] J.-Y. Byeon, R.C. Bailey, *Analyst* 136 (2011) 3430-3433.
- 1000 [140] M.S. Luchansky, R.C. Bailey, *J. Am. Chem. Soc.* 133 (2011) 20500-20506.
- 1001 [141] A.J. Qavi, J.T. Kindt, M.A. Gleeson, R.C. Bailey, *Anal. Chem.* 83 (2011)
1002 5949-5956.

- 1003 [142] M.S. Luchansky, A.L. Washburn, M.S. McClellan, R.C. Bailey, *Lab Chip* 11
1004 (2011) 2042-2044.
- 1005 [143] A.L. Washburn, J. Gomez, R.C. Bailey, *Anal. Chem.* 83 (2011) 3572-3580.
- 1006 [144] A.L. Washburn, M.S. Luchansky, A.L. Bowman, R.C. Bailey, *Anal. Chem.*
1007 82 (2010) 69-72.
- 1008 [145] <http://www.genalyte.com/>
- 1009 [146] J. Escorihuela, M.J. Bañuls, R. Puchades, A. Maquieira, *Chem. Commun.* 48
1010 (2012) 2116-2118.
- 1011 [147] C. Mateo, O. Abian, G. Fernandez-Lorente, J. Pedroche, R. Fernández-
1012 Lafuente, J.M. Guisán, *Biotechnol. Prog.* 18 (2002) 629-634.
- 1013 [148] B. Thierry, M. Jasiénak, L.C.P. de Smet, K. Vasilev, H.J. Griesser, *Langmuir*
1014 24 (2008) 10187-10195.
- 1015 [149] J. Escorihuela, M. J. Bañuls, R. Puchades, A. Maquieira, *Bioconj. Chem.* 23
1016 (2012) 2121-2128.
- 1017 [150] M. Weisser, G. Tovar, S. Mittler-Neher, W. Knoll, F. Brosinger, H. Freimut,
1018 M. Lacher, W. Ehrfeld, *Biosens. Bioelectron.* 14 (1999) 405-411.
- 1019 [151] a) J. Escorihuela, M.J. Bañuls, J.G. Castelló, V. Toccafondo, J. García-
1020 Rupérez, R. Puchades, Á. Maquieira, *Anal. Bioanal. Chem.* 404 (2012) 2831-
1021 2840
- 1022 b) V. Toccafondo, J. García-Rupérez, M.J. Bañuls, A. Griol, J.G. Castelló, S.
1023 Peransi-Llopis, A. Maquieira, *Opt. Lett.* 35 (2010) 3673-3675.
- 1024 [152] J.D. Suter, D.J. Howard, H. Shi, C.W. Caldwell, X. Fa, *Biosens. Bioelectron.*
1025 26 (2010) 1016-1020.
- 1026 [153] J.T. Gohring, P.S. Dale, X. Fang, *Sens. Actuators B* 146 (2010) 226-230.
- 1027 [154] F.F. Bier, F.W. Scheller, *Biosens. Bioelectron.* 11 (1996) 669-678.
- 1028 [155] F.F. Bier, F. Kleinjung, F.W. Scheller, *Sens. Actuators B* 38 (1997) 78-82.
- 1029 [156] <http://www.microvacuum.com/>
- 1030 [157] C.J. Choi, A.R. Belobraydich, L.L. Chan, P.C. Mathias, B.T. Cunningham,
1031 *Anal. Biochem.* 405 (2010) 1-10.
- 1032 [158] I.D. Block, P.C. Mathias, N. Ganesh, S.I. Jones, B.R. Dorvel, V. Chaudhery,
1033 L.O. Vodkin, R. Bashir, B.T. Cunningham, *Opt. Express* 17 (2009) 13222-
1034 13235.
- 1035 [159] J. Shang, F. Cheng, M. Dubey, J.M. Kaplan, M. Rawal, X. Jiang, D.S.
1036 Newburg, P.A. Sullivan, R.B. Andrade, D.M. Ratner, *Langmuir* 28 (2012)
1037 3338-3344.
- 1038 [160] E.L. Hanson, J. Schwartz, B. Nickel, N. Koch, M.F.J. Danisman, *J. Am.*
1039 *Chem. Soc.* 125 (2003) 16074-16080.
- 1040 [161] A. Cattani-Scholz, D. Pedone, F. Blobner, G. Abstreiter, J. Schwartz, M.
1041 Tornow, L. Andruzzi, *Biomacromolecules* 10 (2009) 489-496.
- 1042 [162] F. Cheng, J. Shang, D.M. Ratner, *Bioconjugate Chem.* 22 (2011) 50-57.
- 1043 [163] A. Cattani-Scholz, D. Pedone, M. Dubey, S. Nepl, B. Nickel, P. Feulner, J.
1044 Schwartz, G. Abstreiter, M. Tornow, *ACS Nano* 2 (2008) 1653-1660.
- 1045 [164] K.S. Midwood, M.D. Carolus, M.P. Danahy, J.E. Schwarzbauer, J. Schwartz,
1046 *Langmuir* 20 (2004) 5501-5505.
- 1047 [165] D. Brovelli, G. Hahner, L. Ruiz, R. Hofer, G. Kraus, A. Waldner, J.
1048 Schlosser, P. Oroszlan, M. Ehrat, N.D. Spencer, *Langmuir* 15 (1999) 4324-
1049 4327.
- 1050 [166] <http://www.zeptosens.com>
- 1051 [167] Zeptosens A G, WO 02 020873 A3, 2002.

- 1052 [168] T. Böcking, K.A. Kilian, K. Gaus, J.J. Gooding, *Adv. Funct. Mater.* 18
1053 (2008) 3827-3833.
- 1054 [169] H. Qiao, B. Guan, J.J. Gooding, P. Reece, *Opt. Express* 18 (2010) 15174-
1055 15182.
- 1056 [170] L. De Stefano, L. Rotiroti, I. Rea, I. Rendina, L. Moretti, G. Di Francia, E.
1057 Massera, A. Lamberti, P. Arcadi, C. Sangez, *J. Opt. A: Pure Appl. Opt.* 8
1058 (2006) S540-S544.
- 1059 [171] L. De Stefano, P. Arcadi, A. Lamberti, C. Sanges, L. Rotiroti, I. Rea, I.
1060 Rendina, *Sensors* 7 (2007) 214-221.
- 1061 [172] M.J. Bañuls, V. González-Pedro, C.A. Barrios, R. Puchades, A. Maquieira,
1062 *Biosens. Bioelectron.* 25 (2010) 1460-1466.
- 1063 [173] C.A. Barrios, M.J. Bañuls, V. González-Pedro, K.B. Gylfason, B. Sánchez,
1064 A. Griol, A. Maquieira, H. Sohlström, M. Holgado, R. Casquel, *Optics Lett.*
1065 33 (2008) 708-710.
- 1066 [174] C.F. Carlborg, K.B. Gylfason, A. Kazmierczak, F. Dortu, M.J. Bañuls, A.
1067 Maquieira, G.M. Kreshbach, H. Sohlstrom, T. Moh, L. Vivien, J. Popplewel,
1068 G. Ronan, C.A. Barrios, G. Stemme, W. van deer Wijngaart, *Lab Chip* 10
1069 (2010) 281-290.
- 1070 [175] J. Goddard, S. Mandal, D. Erickson, in: X. Fan (Ed.), *Advanced Photonic*
1071 *Structures for Biological and Chemical Detection*; Springer, New York, 2009,
1072 Vol III, pp 445-470.
- 1073 [176] J. Satija, V.V.R. Sai, S. Mukherji, *J. Mater. Chem.* 21 (2011) 14367-14386.
- 1074 [177] F. Vollmer, S. Arnold, D. Braun, I. Teraoka, A. Libchaber, *Biophys. J.* 85
1075 (2003) 1974-1979.
- 1076 [178] J. Adrian, S. Pasche, J.-M. Diserens, F. Sánchez-Baeza, H. Gao, M.P. Marco,
1077 G. Voirin, *Biosens. Bioelectron.* 24 (2009) 3340-3346.
- 1078 [179] G.L. Bratthauer, in: L. C. Javois Ed., *Immunocytochemical Methods and*
1079 *Protocols*, Humana Press: Totowa, NJ, USA, 1995
- 1080 [180] G.T. Hermanson, *Bioconjugate Techniques*, 2nd Ed. Academic Press, London
1081 UK, 2008, pp 900-924
- 1082 [181] M.S. Luchansky, A.I. Washburn, T.A. Martin, M. Iqbal, L.C. Gunn, R.C.
1083 Bailey, *Biosens. Bioelectron.* 26 (2010) 1283-1291.
- 1084 [182] M. Bras, V. Dugas, F. Bessueille, J.P. Cloarec, J.R. Martin, M. Cabrera, J.P.
1085 Chauvet, E. Souteyrand, M. Garrigues, *Biosens. Bioelectron.* 20 ((2004)
1086 797-806.
- 1087 [183] D. Mira, R. Llorente, S. Morais, R. Puchades, A. Maquieira, J. Martí, *Proc.*
1088 *SPIE-Int. Soc. Opt. Eng.* 56 (2004), 364-369.
- 1089 [184] A.M. Armani, R.P. Kulkarni, S.E. Fraser, R.C. Flagan, K.J. Vahala, *Science*
1090 317 (2007) 783-787.
- 1091 [185] S. Mandal, D. Erickson, *Opt. Express* 16 (2008) 1623-1631.
- 1092 [186] S. Mandal, R. Akhmechet, L. Chen, S. Nugen, A. Baumeuer, D. Erickson,
1093 *Proced. SPIE* 6645 (2007) 66451J
- 1094 [187] M.A. Caipa Campos, J.M.J. Paulasse, H. Zuilhof, *Chem. Commun.* 46 (2010)
1095 5512-5515.
- 1096 [188] L.G. Carrascosa, S. Gómez-Montes, A. Aviñó, A. Nadal, M. Pla, R. Eritja,
1097 L.M. Lechuga, *Nucl. Acids Res.* 40 (2012) e56.
- 1098 [189] T. Kodadek, M.M. Reddy, H.J. Olivos, K. Bachhawat-Sikder, P.G. Alluri,
1099 *Acc. Chem. Res.* 37 (2004) 711-718.
- 1100 [190] K. Sefah, J.A. Phillips, X. Xiong, L. Meng, D. Van Simaey, H. Chen, J.
1101 Martin, W. Tan, *Analyst* 134 (2009) 1765-1775.

1102 [191] H.D. Agnew, R.D. Rohde, S.W. Millward, A. Nag, W.-S. Yeo, J.E. Hein,
1103 S.M. Pitram, A.A. Tariq, V.M. Burns, R.J. Krom, V.V. Fokin, K.B.
1104 Sharpless, J.R. Heath, *Angew. Chem. Int. Ed.* 48 (2009) 4944-4948.
1105
1106
1107

1108 **Figure Captions**

1109

1110 **Figure 1:** Number of publications per year on the Refractive Index Optical BioSensing
1111 topic during the last decade.

1112 **Figure 2:** Scheme of the most relevant functionalization procedures on silicon-based
1113 materials for IO biosensors: organosilane-based (a), phosphonate-based (b), and
1114 glutaraldehyde-based (c) approaches.

1115 **Figure 3:** Scheme of the bioconjugation procedures employed in IO biosensors for
1116 aminated surfaces: N-hydroxysuccinimide-based (a), succinic anhydride-based (b), p-
1117 phenylenediisocyanate-based (c), glutaraldehyde-based (d) hydrazine-aldehyde-based
1118 (e) and carboxy-ended dendrimer-based (f) approaches.

1119 **Figure 4:** Scheme of the bioconjugation procedures employed in IO biosensors for
1120 thiol-ended surfaces: disulfide bridge-based (a), m-maleimidobenzoyl-N-
1121 hydroxysuccinimide-based (b) and thiol-ended click chemistry-based (c) approaches.

1122 **Figure 5:** Scheme of the bioconjugation procedures employed in IO biosensors for
1123 epoxy-ended surfaces: nucleophilic ring opening-based (a), oxidative ring opening-
1124 based (b) and photo-induced ring opening-based (c) approaches.

1125 **Figure 6:** Scheme of the bioconjugation procedures for the carboxylated surfaces (a)
1126 and isocyanate-ended surfaces (b), employed in IO biosensors.

1127 **Figure 7:** Some examples of IO biosensors characterizations: a) Comparison between
1128 intensity of fluorescence in a microarray of a Cy5-labeled antibody (same
1129 concentration) deposited onto a silicon (left) and a silicon oxide (right) surface; b) SEM
1130 images of the slot waveguides with streptavidin selectively attached on silicon nitride
1131 following the chemical approach shown in Figure 2.c; c) Fluorescence confocal
1132 microscopy characterization for the SiN slot waveguides modified according to the
1133 procedure shown in Figure 2c, and using the Cy5-labeled antibody and 1% Fluorescein

1134 isothiocyanate as a contrast; d) ToF-SIMS measurements (CN⁻ and CNO⁻ ions) on the
1135 waveguides functionalized with isocyanate-ended organosilane (red arrows show the
1136 defects on the organosilane layer formed on the surface), e) layout of an RI IO biosensor
1137 consisting of seven slot waveguide ring resonators, six sensing rings and a reference
1138 ring, a microscope image of a reference and a sensing ring (with an open window in the
1139 sensing area) and a measurement scheme.

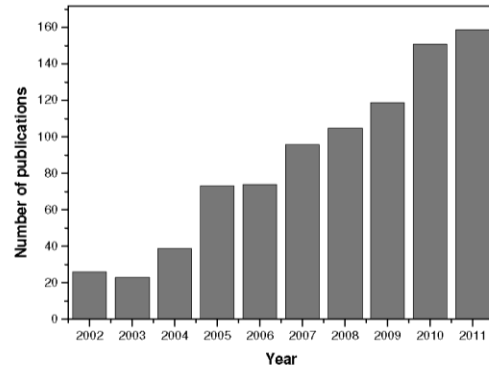
1140

1141

1142

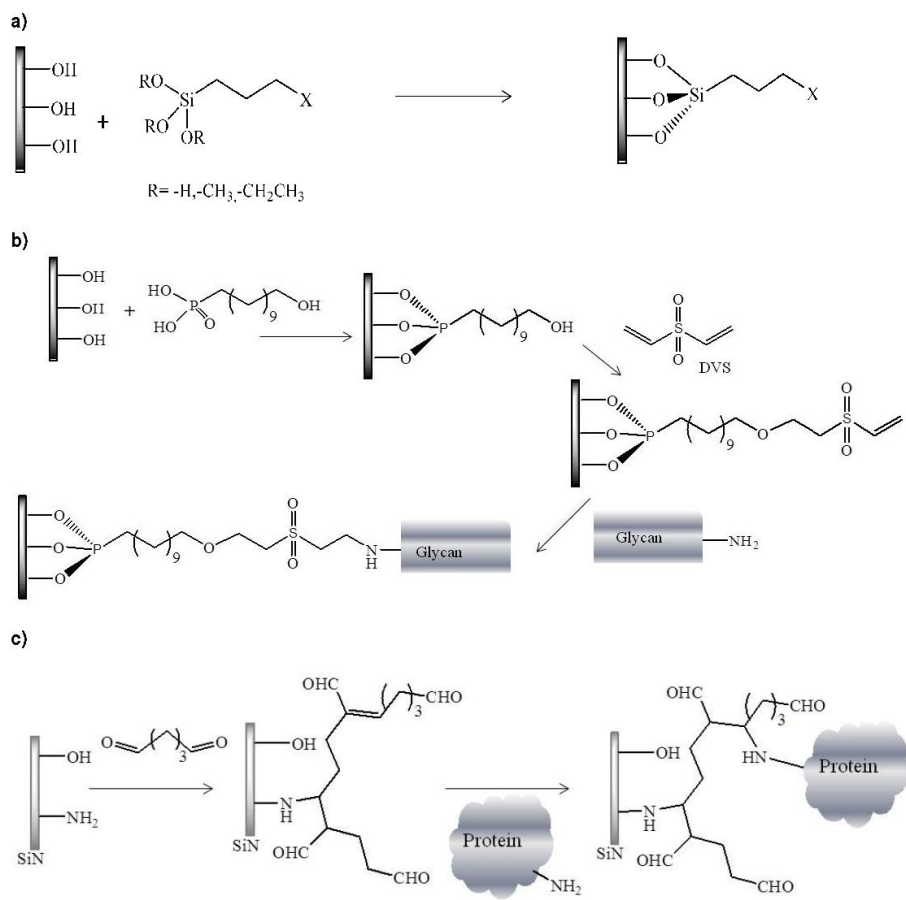
1143 **Figures:**

Figure 1



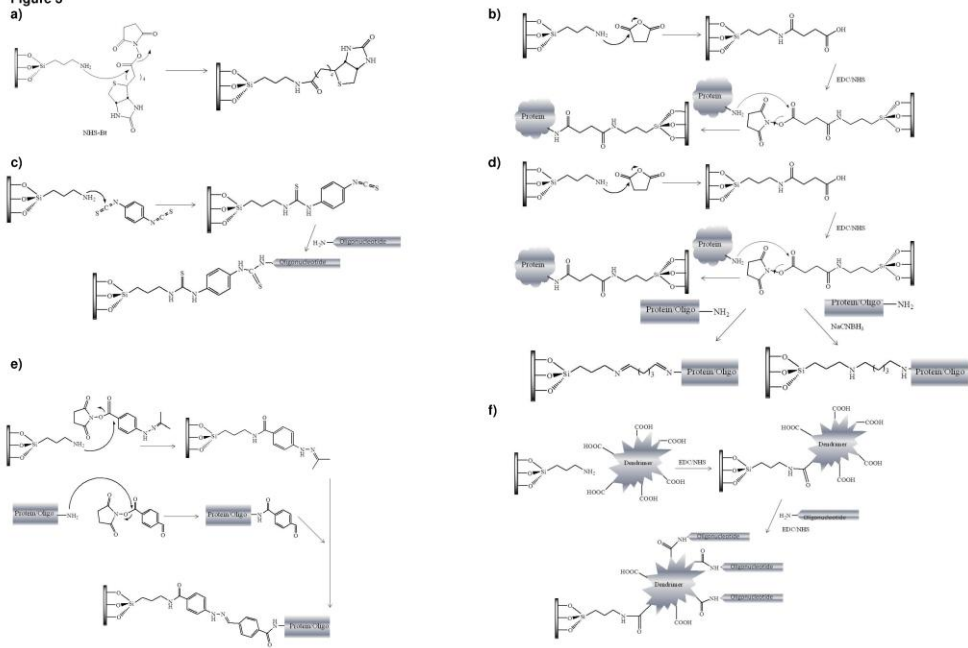
1144
1145

Figure 2



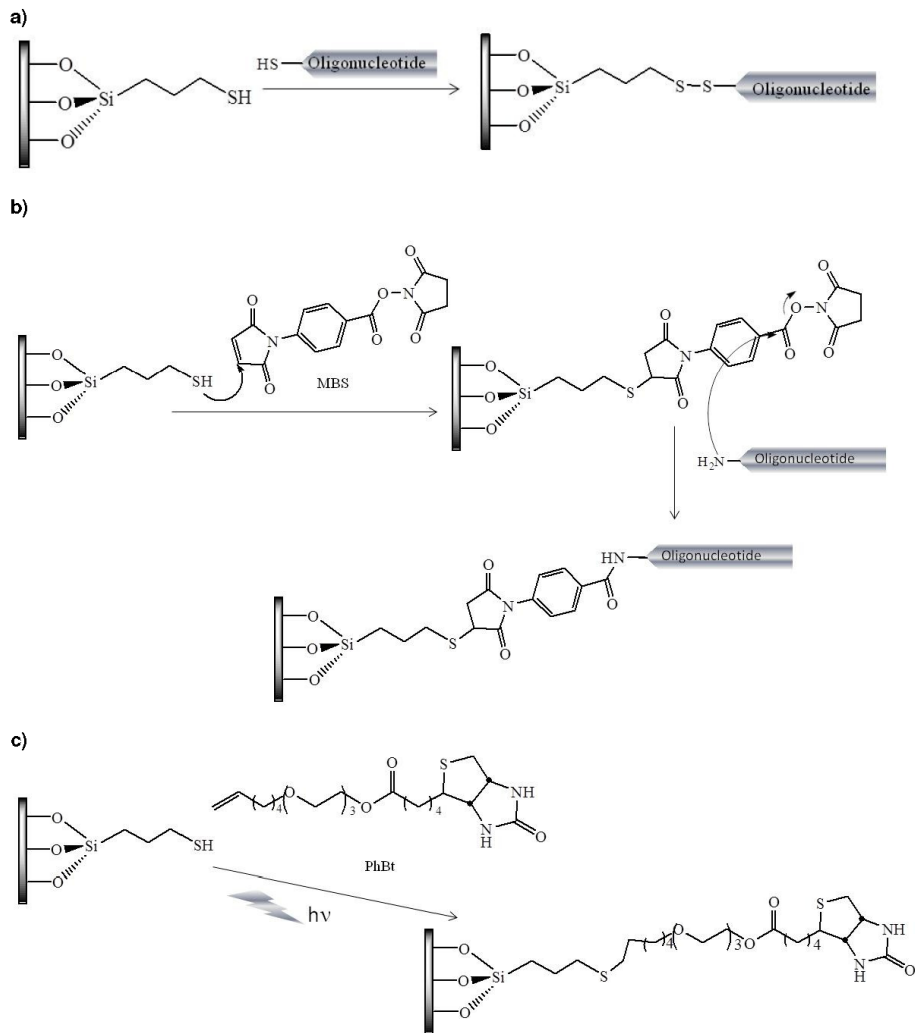
1146
1147

Figure 3



1148
1149

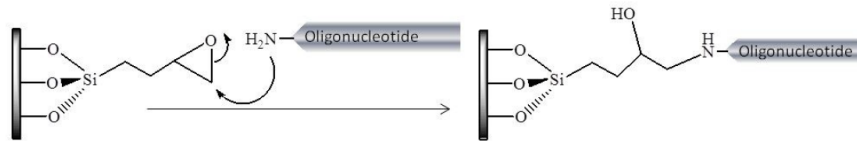
Figure 4



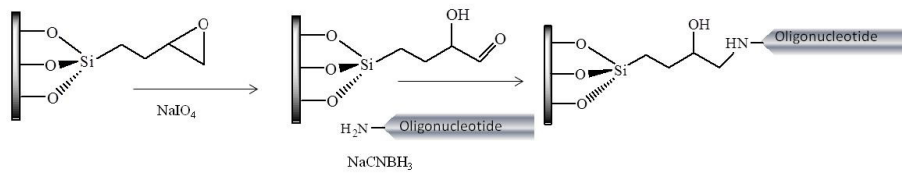
1150
1151

Figure 5

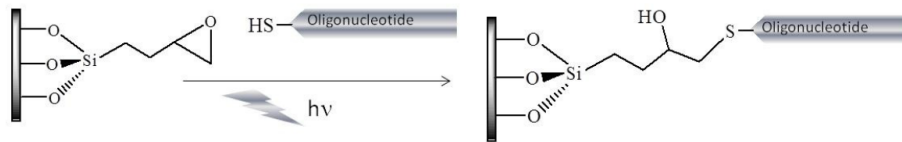
a)



b)



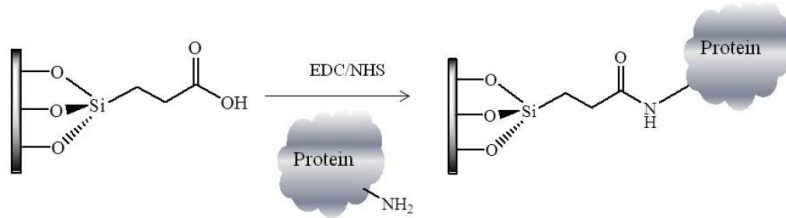
c)



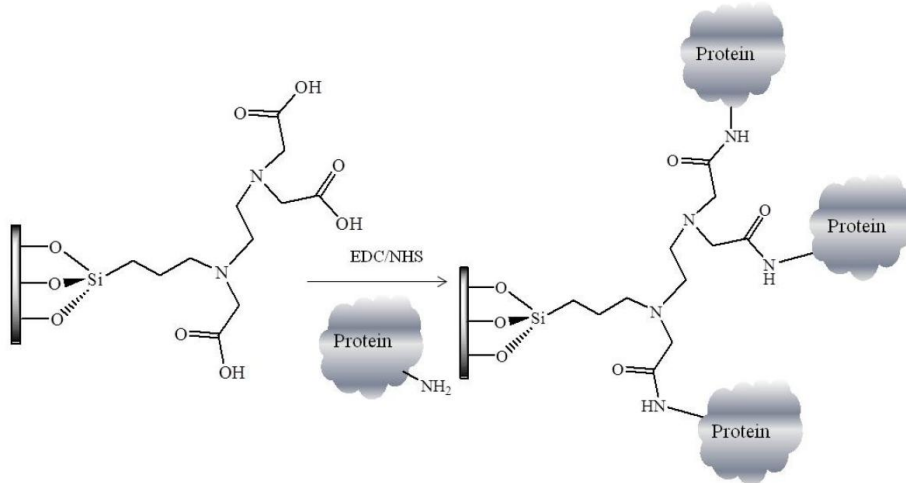
1152
1153

Figure 6

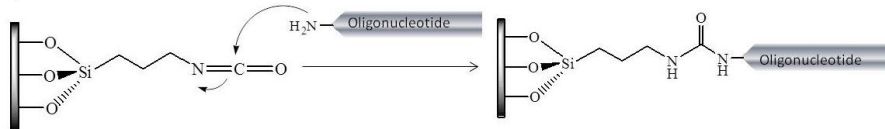
a.1)



a.2)



b)



1154
1155

Figure 7

